Polymer 49 (2008) 4469–4474

Contents lists available at ScienceDirect

Polymer

journal homepage: www.elsevier.com/locate/polymer

Closed miscibility loop phase behavior of polymer solutions

Suk Yung Oh, Young Chan Bae*

Division of Chemical Engineering and Molecular Thermodynamics Laboratory, Hanyang University, Seoul 133-791, Republic of Korea

ARTICLE INFO

Article history:
Received 26 June 2008
Received in revised form 30 July 2008
Accepted 31 July 2008
Available online 3 August 2008

Keywords:
Modified double lattice model
Liquid–liquid equilibria
Closed miscibility loop

ABSTRACT

In our previous study, we proposed a modified double lattice model, which is capable of describing and predicting the phase equilibria of binary polymer solutions. The model successfully describes the liquid–liquid equilibria having an upper critical solution temperature (UCST) and a lower critical solution temperature (LCST), but cannot predict the closed miscibility loop phase behavior. The closed miscibility loop phase behavior may be mainly due to highly specific interactions such as hydrogen bonding. The purpose of this study is to extend our previous model to describe closed miscibility loop phase behavior by employing a new specific interaction term to account for highly specific interactions. According to the proposed model, quantitative description is in good agreement with experimental data and gives improved results when compared with those of other methods.

1. Introduction

Most common phase behaviors of binary polymer/solvent mixtures are upper critical solution temperature (UCST), lower critical solution temperature (LCST), hour-glass shaped and closed miscibility loop types. In closed miscibility loop behaviors of binary polymer solutions, the specific oriented interaction is energetically favored because the energy is lowered upon pair formation. However, it is entropically unfavored because the number of configurations characteristic of the nonspecific interaction outweighs the number of configurations characteristic of the specific oriented interaction.

A number of thermodynamic models attempt to deal specifically with closed loop mixtures. Firstly, Barker and Fock [1] give a qualitative description of a closed loop coexistence curve for a binary system. In Barker's associated solutions, the multiple interaction sites of the lattice points with different and temperature independent energies were incorporated to explain the closed loop behaviors. However, the model cannot describe that binary system quantitatively. The first successful non-mean-field method for describing the miscibility loop was developed by Wheeler [2] and Anderson and Wheeler [3]. Their decorated lattice model can be mapped onto a three-dimensional Ising model for which reliable solutions are available. Although the Ising statistics are unfamiliar and the procedure is too complicated for practical purpose, the decorated lattice model obtained qualitative agreement between calculated and experimental coexistence curves for several binary low-molecular-weight systems. Wheeler's theory was incorporated into the UNIQUAC equation [4] by Kim and Kim [5]. They developed a decorated lattice model by using two step approximations of local compositions and the orientational effect of interacting sites. Their model reproduced temperature–composition diagrams which are closed loop, fairly well; however, the model cannot describe quantitatively, too. A Flory–Huggins based model to describe closed loop behavior has also been proposed. Matsuyama and Tanaka [6], Vause and Walker [7] and Bae et al. [8] reported a simple method to represent phase equilibria for the miscibility closed loop behaviors of binary polymer solutions. Recently, Yang et al. [9–12] developed a new lattice model for polymer solutions by combining the molecular simulation with statistical mechanics, several types of phase diagrams such as UCST, LCST, and miscibility loop diagrams are described.

To account for highly oriented interactions, Hu et al. [13,14] established a double lattice model with secondary lattice concept. Using four adjustable parameters, coexistence curves are fitted well for systems having a miscibility loop. Hino et al. [15] also obtained a closed loop temperature composition phase diagram adopting the incompressible lattice-gas model by Brinke and Karasz [16] to introduce the effect of specific interactions into a recently presented Monte-Carlo-based lattice expression for the Helmholtz energy of nonrandom mixing. At present all of the published models provide a qualitative description of a closed loop coexistence curves, but these models cannot describe large variety of systems quantitatively.

Oh and Bae [17] modified Hu's double lattice model by introducing a new interaction parameter and simplifying the expression of the Helmholtz energy of mixing. In this study, we describe the

* Corresponding author. Tel.: +82 2 2220 0529; fax: +82 2 2296 0568.
E-mail address: ycbae@hanyang.ac.kr (Y.C. Bae).
URL: http://www.inchem.hanyang.ac.kr/lab/mtl

0032-3861/$ – see front matter © 2008 Elsevier Ltd. All rights reserved.
doi:10.1016/j.polymer.2008.07.055

liquid–liquid phase equilibria of the binary polymer solution, using a modified double lattice model. To take into account strong specific interaction, we revise a secondary lattice term with additional temperature dependent energy contribution.

2. Model development

2.1. Modified double lattice model

The framework of the lattice model starts with a simple cubic lattice (coordination number $z=6$) containing N_r sites. The systems (two different polymer chains, polymer/solvent systems, *etc.*) that interact strongly must be in the correct orientation to each other, *i.e.*, a specific interaction. Ordinary polymer solutions are described by the primary lattice, while a secondary lattice is introduced as a perturbation to account for oriented interactions.

2.1.1. Primary lattice

Oh and Bae [17] defined a new Helmholtz energy of mixing in the form of the Flory–Huggins theory. The expression is given by

$$\frac{\Delta A}{N_r kT} = \left(\frac{\phi_1}{r_1}\right)\ln\phi_1 + \left(\frac{\phi_2}{r_2}\right)\ln\phi_2 + \chi_{OB}\phi_1\phi_2 \tag{1}$$

where N_r is the total number of lattice sites (coordination number $z=6$), k is the Boltzmann constant, r_i is the number of segments, and ϕ_i is the volume fraction of component i. The subscripts 1 and 2 refer to the solvent and polymer, respectively. χ_{OB} is a new interaction parameter defined by

$$\chi_{OB} = C_\beta\left(\frac{1}{r_2}-\frac{1}{r_1}\right)^2 + \left(2+\frac{1}{r_2}\right)\tilde{\varepsilon} - \left(\frac{1}{r_2}-\frac{1}{r_1}+C_\gamma\tilde{\varepsilon}\right)\tilde{\varepsilon}\phi_2 + C_\gamma\tilde{\varepsilon}^2\phi_2^2 \tag{2}$$

where C_β and C_γ are universal constants. These constants are determined by comparing with Madden et al.'s Monte-Carlo simulation data [18]. The best-fit values of C_β and C_γ are 0.1415 and 1.7986, respectively.

$\tilde{\varepsilon}$ is a reduced interaction energy parameter given by

$$\tilde{\varepsilon} = \frac{\varepsilon}{kT} = \frac{\varepsilon_{11}+\varepsilon_{22}-2\varepsilon_{12}}{kT} \tag{3}$$

where ε_{11}, ε_{22} and ε_{12} are for the corresponding nearest neighbor segment–segment interactions. We define the above model as Model I in this study. In the case of describing UCST curves, we use Model I because the specific interaction is very weak in that system.

2.1.2. Secondary lattice

To improve the mathematical approximation defect and to reduce the number of parameters, a new Helmholtz energy of mixing as the fractional form is defined. The expression is given by

$$\frac{\Delta A_{sec,ij}}{N_{ij,kT}} = \frac{2}{z}\left[\eta\ln\eta + (1-\eta)\ln(1-\eta) + \frac{zC_\alpha\delta\tilde{\varepsilon}_{ij}(1-\eta)\eta}{1+C_\alpha\delta\tilde{\varepsilon}_{ij}(1-\eta)\eta}\right] \tag{4}$$

where $\Delta A_{sec,ij}$ is the Helmholtz energy of mixing of the secondary lattice for i–j segment–segment pair and N_{ij} is the number of i–j pairs, $\delta\tilde{\varepsilon}(\delta\varepsilon/kT)$ is the reduced energy parameter contributed by the oriented interactions and η is the surface fraction permitting oriented interactions. For simplicity, we arbitrarily set η to 0.3 as suggested by Hu et al. [13] C_α is a universal constant that is determined by comparing with Panagiotopolous et al.'s Gibbs-ensemble Monte-Carlo simulation data of the Ising lattice [19]. The best-fit value of C_α is 0.4881. We define this as Model II, and in the case of describing LCST curves, we use Model II to deal with the specific interaction. For aqueous polymer solutions having a closed miscibility loop, strong specific interactions increase with increasing temperatures. Therefore, $\delta\varepsilon$ is separated into two parts to take the temperature dependence into account. We replace $\delta\varepsilon$ by $\delta\varepsilon^H - \delta\varepsilon^S T$ in Eq. (4) where $\delta\varepsilon^H$ and $\delta\varepsilon^S$ are enthalpic and entropic energy contributions for the oriented interactions, respectively. Two parameters represent the enthalpic disadvantage, $\delta\varepsilon^H$, and the entropic advantage, $\delta\varepsilon^S$, for $\delta\varepsilon$ when system temperature increases. This is Model III in this study.

2.1.3. Incorporation of secondary lattice into primary lattice

To incorporate a secondary lattice, we replace ε_{ij} by $\varepsilon^{ij} - (\Delta A_{sec,ij}/N_{ij})$ in Eq. (3). If oriented interaction occurs in the i–j segment–segment pairs, we replace $\tilde{\varepsilon}$ by $(\varepsilon/kT) + 2(\Delta A_{sec,ij}/N_{ij}kT)$ in Eq. (3). If oriented interaction occurs in the i–i segment–segment pairs, we replace $\tilde{\varepsilon}$ by $\varepsilon/kT - (\Delta A_{sec,ij}/N_{ii}kT)$. In this study, we assume that the oriented interaction occurs only in the i–j segment–segment pairs.

2.2. Correlating equations

For calculating the binary coexistence curve, we need the chemical potential of components 1 and 2. They are given by

$$\frac{\Delta\mu_1}{kT} = \ln(1-\phi_2) - r_1\left(\frac{1}{r_2}-\frac{1}{r_1}\right)\phi_2 + r_1\left[C_\beta\left(\frac{1}{r_2}-\frac{1}{r_1}\right)^2 + \left(\left(\frac{1}{r_2}-\frac{1}{r_1}\right)+C_\gamma\tilde{\varepsilon}\right)\tilde{\varepsilon} + \left(2+\frac{1}{r_2}\right)\tilde{\varepsilon}\right]\phi_2^2 - 2r_1\left[\left(\left(\frac{1}{r_2}-\frac{1}{r_1}\right)+C_\gamma\tilde{\varepsilon}\right)\tilde{\varepsilon} + C_\gamma\tilde{\varepsilon}^2\right]\phi_2^3 + 3r_1C_\gamma\tilde{\varepsilon}^2\phi_2^4 \tag{5}$$

$$\frac{\Delta\mu_2}{kT} = \ln\phi_2 + r_2\left[\left(\frac{1}{r_2}-\frac{1}{r_1}\right) + C_\beta\left(\frac{1}{r_2}-\frac{1}{r_1}\right)^2 + \left(2+\frac{1}{r_2}\right)\tilde{\varepsilon}\right] - r_2\left[\left(\frac{1}{r_2}-\frac{1}{r_1}\right) + 2\left(\left(\frac{1}{r_2}-\frac{1}{r_1}\right)+C_\gamma\tilde{\varepsilon}\right)\tilde{\varepsilon} + 2C_\beta\left(\frac{1}{r_2}-\frac{1}{r_1}\right)^2 + 2\left(2+\frac{1}{r_2}\right)\tilde{\varepsilon}\right]\phi_2 + r_2\left[4\left(\left(\frac{1}{r_2}-\frac{1}{r_1}\right)+C_\gamma\tilde{\varepsilon}\right)\tilde{\varepsilon} + \left(2+\frac{1}{r_2}\right)\tilde{\varepsilon} + C_\beta\left(\frac{1}{r_2}-\frac{1}{r_1}\right)^2 + 3C_\gamma\tilde{\varepsilon}^2\right]\phi_2^2 - r_2\left[6C_\gamma\tilde{\varepsilon}^2 + 2\left(\left(\frac{1}{r_2}-\frac{1}{r_1}\right)+C_\gamma\tilde{\varepsilon}\right)\tilde{\varepsilon}\right]\phi_2^3 + 3r_2C_\gamma\tilde{\varepsilon}^2\phi_2^4 \tag{6}$$

The coexistence curve is found from the following conditions:

$$\Delta\mu_1' = \Delta\mu_1'' \tag{7}$$

$$\Delta\mu_2' = \Delta\mu_2'' \tag{8}$$

where $\Delta\mu_i$ is the change in chemical potential upon isothermally transferring component i from the pure state to the mixture. Superscripts $'$ and $''$ denote two phases at equilibrium. For phase equilibrium calculation, we require the experimental coordinates of the critical point. And the critical condition is given by

$$\frac{\partial^2(\Delta A/N_r kT)}{\partial\phi_2^2} = \frac{-1}{1-\phi_2} - r_1\left(\frac{1}{r_2}-\frac{1}{r_1}\right) + 2r_1\left(C_\beta\left(\frac{1}{r_2}-\frac{1}{r_1}\right)^2 + \left(\left(\frac{1}{r_2}-\frac{1}{r_1}\right)+C_\gamma\tilde{\varepsilon}\right)\tilde{\varepsilon} + \left(2+\frac{1}{r_2}\right)\tilde{\varepsilon}\right)\phi_2 - 6r_1\left(\left(\left(\frac{1}{r_2}-\frac{1}{r_1}\right)+C_\gamma\tilde{\varepsilon}\right)\tilde{\varepsilon}+C_\gamma\tilde{\varepsilon}^2\right)\phi_2^2 + 12r_1C_\gamma\tilde{\varepsilon}^2\phi_2^3 = 0 \quad (9)$$

and

$$\frac{\partial^3(\Delta A/N_r kT)}{\partial\phi_2^3} = \frac{-1}{(1-\phi_2)^2} + 2r_1\left(C_\beta\left(\frac{1}{r_2}-\frac{1}{r_1}\right)^2 + \left(\left(\frac{1}{r_2}-\frac{1}{r_1}\right)+C_\gamma\tilde{\varepsilon}\right)\tilde{\varepsilon} + \left(2+\frac{1}{r_2}\right)\tilde{\varepsilon}\right) - 12r_1\left(\left(\left(\frac{1}{r_2}-\frac{1}{r_1}\right)+C_\gamma\tilde{\varepsilon}\right)\tilde{\varepsilon}+C_\gamma\tilde{\varepsilon}^2\right)\phi_2 + 36r_1C_\gamma\tilde{\varepsilon}^2\phi_2^2 = 0 \quad (10)$$

3. Results and discussion

For ordinary binary mixtures we introduce the primary lattice model (Model I) to obtain a satisfactory fit to describe UCST curves. For the systems (two different polymer chains, polymer–solvent system, *etc.*) that interact strongly, they must be in the proper orientation to each other (*i.e.*, a specific interaction). These systems show the LCST phase behavior, which the primary lattice alone cannot describe. Therefore, to describe this phenomenon, we introduce a secondary lattice (Model II). In particular, for systems having closed miscibility loops with both UCST and LCST, Model II cannot describe entire shape. Therefore, we introduce the corrected specific interaction model (Model III), which has an additional temperature dependent energy contribution. Table 1 gives a brief summary of the three model types.

Fig. 1 shows phase diagrams of data for polyisobutylene in diisobutyl ketone system [21] in which only upper critical solution temperature data are compared, since specific interaction is not considered. The solid lines are calculated by Model I. As shown in Fig. 1, the calculated curves agree very well with experimental data. The model adjustable parameter values are $r_2 = 145.84$ and $\varepsilon/k = 84.541$ K for a PIB molecular weight of 22 700; $r_2 = 1175.6$ and $\varepsilon/k = 83.655$ K for a PIB molecular weight of 285 000; $r_2 = 6896.3$ and $\varepsilon/k = 83.468$ K for a PIB molecular weight of 6 000 000. In this system, as the molecular weight increases, the values of r_2 also reasonably increase. However, values of ε/k depend weakly on the chain length of the polymer. Model I alone always yields a narrower coexistence curve than experimental data because the specific interaction is not considered in this case.

Fig. 2 shows coexistence curves for polystyrene (PS)/ethyl acetate systems [8] and these systems exhibit LCST behaviors. In this case, we introduce the secondary lattice to account for specific interaction. The solid lines are calculated by Model II. The calculated results agree very well with the experimental data. The model adjustable parameter values are $r_2 = 117.08$, $\varepsilon/k = -875.57$ K and $\delta\varepsilon/k = 8914.7$ K for a PS molecular weight of 100 000; $r_2 = 372.17$, $\varepsilon/k = -788.08$ K and $\delta\varepsilon/k = 7165.8$ K for a PS molecular weight of 223 000; $r_2 = 1257.5$, $\varepsilon/k = 1179.0$ K and $\delta\varepsilon/k = -1427.4$ K for a PS molecular weight of 600 000. Fig. 3 shows coexistence curves for polymethylmethacrylate (PMMA)/tetrahydrofuran (THF) systems [18] and those systems also exhibit LCST behaviors. The solid lines are calculated by Model II. The calculated results also agree well

Table 1
Brief summary of the three model types

Model	LLE type	Model parameter
Model I	UCST	r_2, ε
Model II	LCST	r_2, ε, $\delta\varepsilon$
Model III	Closed loop both UCST and LCST	r_2, ε, $\delta\varepsilon^H$, $\delta\varepsilon^S$

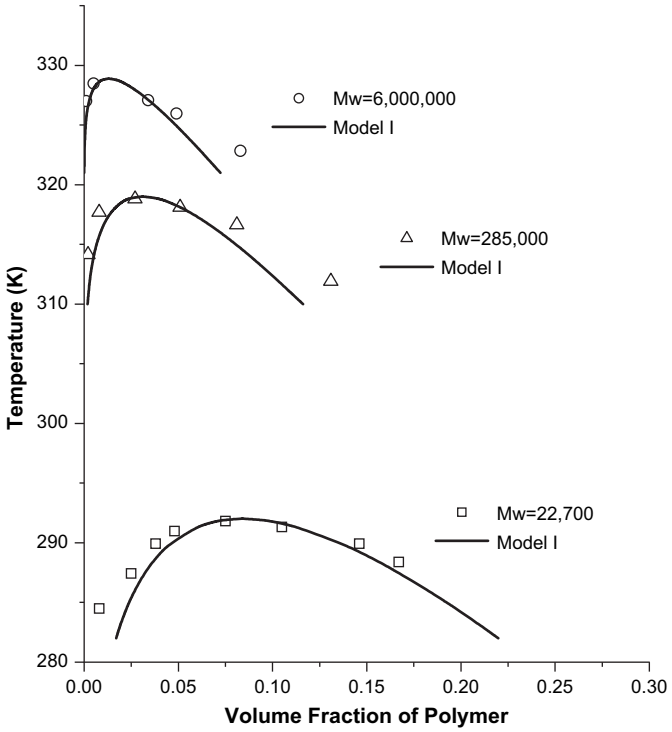

Fig. 1. Coexistence curves for PIB/diisobutyl ketone systems. The open squares, triangles and circles are experimental data [21] for PIB molecular weights of 22 700, 285 000, 6 000 000, respectively. The solid lines are calculated by Model I.

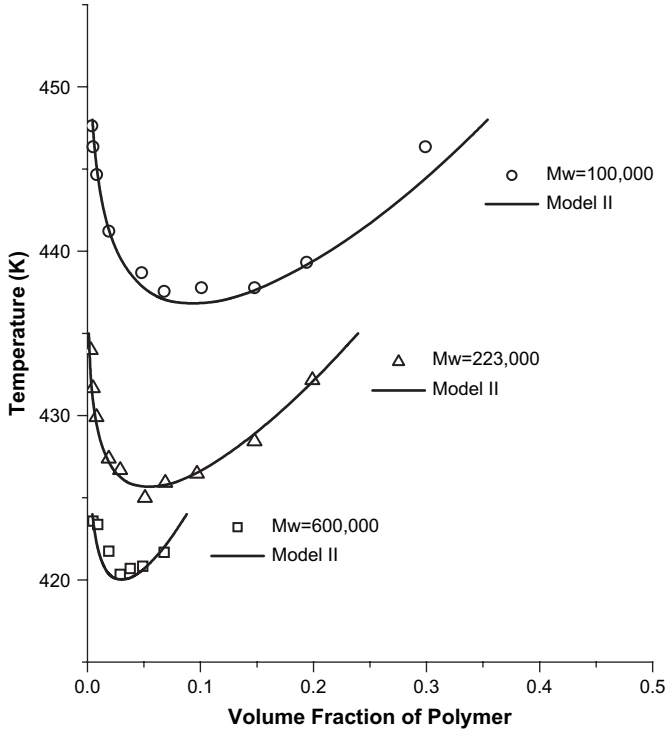

Fig. 2. Coexistence curves for PS/ethyl acetate systems. The open squares, triangles and circles are experimental data [8] for PS molecular weights of 600 000, 223 000, 100 000, respectively. The solid lines are calculated by Model II.

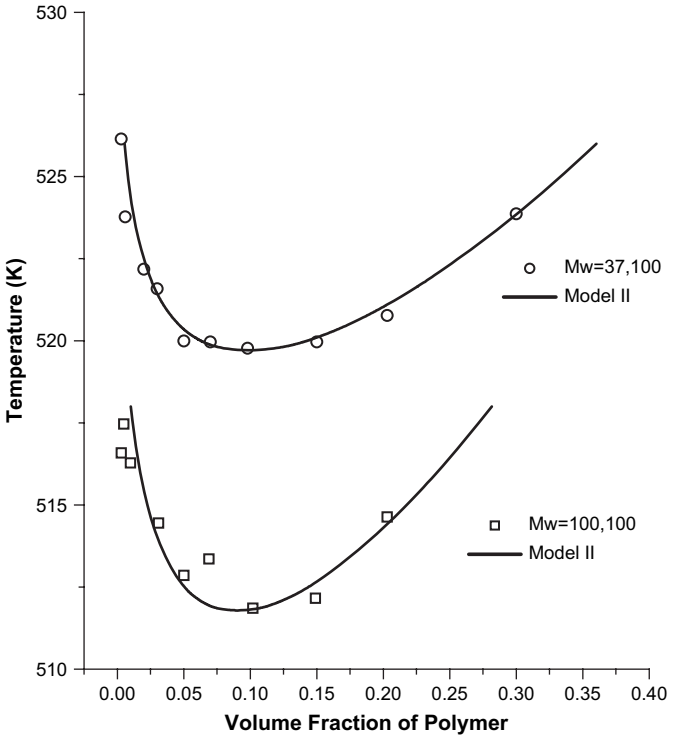

Fig. 3. Coexistence curves for PMMA/THF systems. The open squares and circles are experimental data [22] for PMMA molecular weights of 100 100, 37 100, respectively. The solid lines are calculated by Model II.

with the experimental data. The model adjustable parameter values are $r_2 = 104.50$, $\varepsilon/k = -1437.3$ K and $\delta\varepsilon/k = 33\,219$ K for a PMMA molecular weight of 37 100; $r_2 = 125.69$, $\varepsilon/k = -1140.7$ K and $\delta\varepsilon/k = 13\,656$ K for a PMMA molecular weight of 100 100.

Fig. 4 shows the coexistence curves for polystyrene (PS)/*tert*-butyl acetate systems [20] which has both UCST and LCST. This type of phase diagram consists of two curves which have their own UCST and LCST, respectively. Corrected specific interaction model (Model III) is needed in this case. The model adjustable parameter values are $r_2 = 125.70$, $\varepsilon/k = 358.31$ K, $\delta\varepsilon^H/k = 8287.2$ K and $\delta\varepsilon^S/k = 13.659$ K for a PS molecular weight of 100 000; $r_2 = 222.00$, $\varepsilon/k = 365.25$ K, $\delta\varepsilon^H/k = 8300.4$ K and $\delta\varepsilon^S/k = 13.687$ K for a PS molecular weight of 233 000; $r_2 = 1175.7$, $\varepsilon/k = 290.55$ K, $\delta\varepsilon^H/k = 4234.0$ K and $\delta\varepsilon^S/k = 5.7599$ K for a PS molecular weight of 600 000. Calculated curves also fit fairly well to experiment.

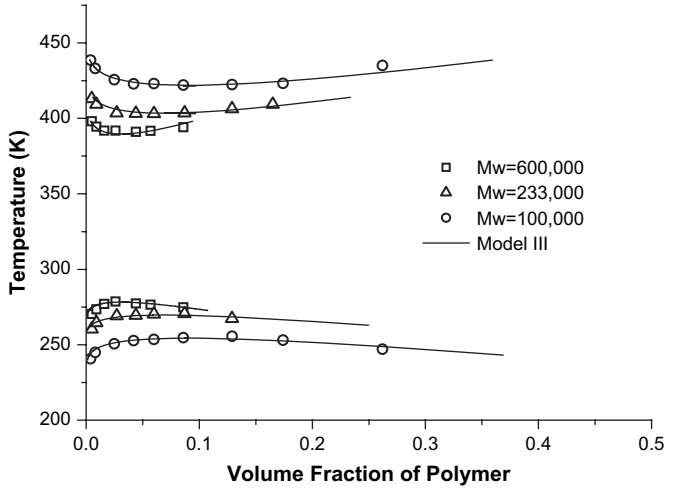

Fig. 4. Coexistence curves for PS/*tert*-butyl acetate systems. The open squares, triangles and circles are experimental data [20] for PS molecular weights of 600 000, 233 000, 100 000, respectively. The solid lines are calculated by Model III.

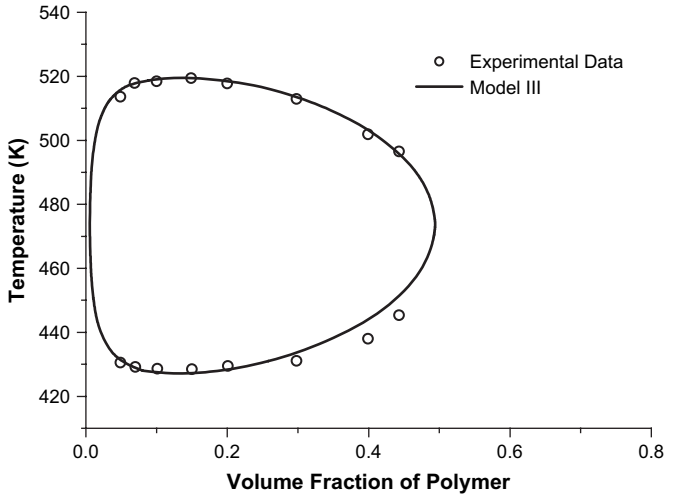

Fig. 5. Coexistence curves for PEG/water system. The open circles are experimental data [20] for PEG molecular weights of 3350. The solid lines are calculated by Model III.

Figs. 5–10 show the calculated and experimental results for aqueous polymer solutions having a closed miscibility loop. In these systems, the specific interaction energy values are very sensitive to temperature change. Therefore, we use a corrected specific interaction model (Model III) to describe phase diagrams.

Figs. 5–7 show the phase diagram of polyethylene glycol (PEG) in water systems [20] and these systems exhibit a closed loop behaviors. The solid lines are calculated by Model III. In these figures, the calculated results by Model III agree well with experimental data. However, for the higher concentration range of PEG it shows a slight deviation between calculated values and experimental data. The model adjustable parameter values are $r_2 = 55.097$, $\varepsilon/k = -1029.1$ K, $\delta\varepsilon^H/k = 35\,809$ K and $\delta\varepsilon^S/k = 48.342$ K for a PEG molecular weight of 3350 (Fig. 5); $r_2 = 91.793$, $\varepsilon/k = -879.64$ K, $\delta\varepsilon^H/k = 18\,710$ K and $\delta\varepsilon^S/k = 20.581$ K for a PEG molecular weight of 8000 (Fig. 6); $r_2 = 149.65$, $\varepsilon/k = -875.10$ K, $\delta\varepsilon^H/k = 18\,168$ K and $\delta\varepsilon^S/k = 19.440$ K for a PEG molecular weight of 15 000 (Fig. 7). As shown in Figs. 5–7, r_2 and ε/k increase with molecular weight of PEG, while $\delta\varepsilon^H/k$ and $\delta\varepsilon^S/k$ decrease with molecular weight of PEG. It shows that energy values are slightly

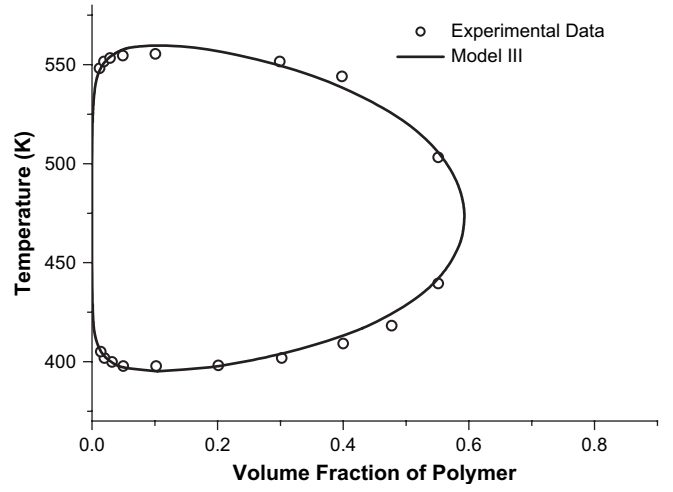

Fig. 6. Coexistence curves for PEG/water system. The open circles are experimental data [20] for PEG molecular weights of 8000. The solid lines are calculated by Model III.

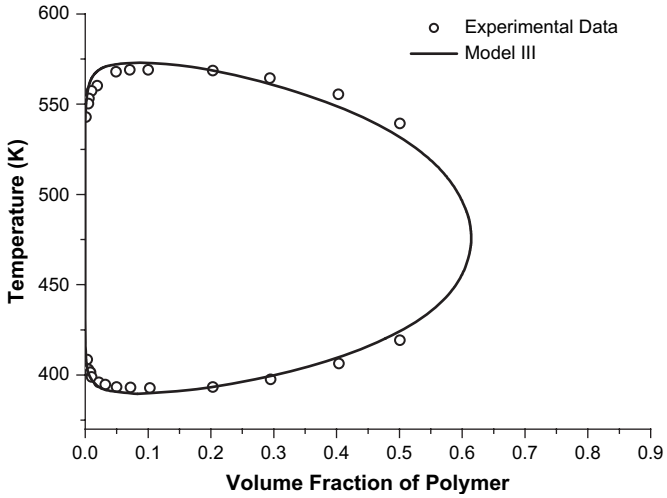

Fig. 7. Coexistence curves for PEG/water system. The open circles are experimental data [20] for PEG molecular weights of 8000. The solid lines are calculated by Model III.

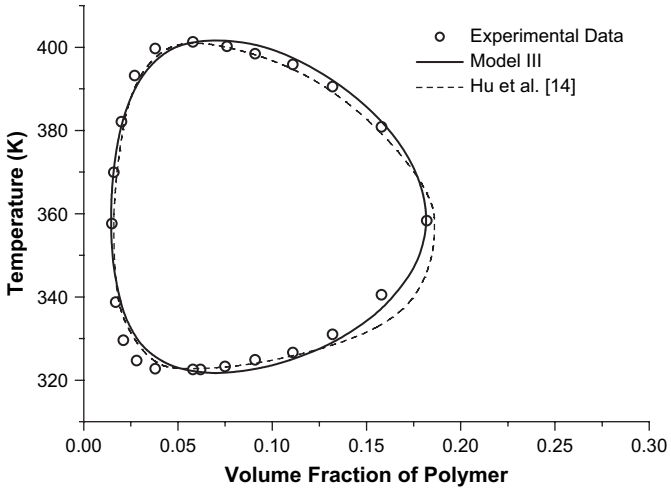

Fig. 9. Coexistence curves for 2-butoxyethanol/water system. The open circles are experimental data [23]. The solid and dashed lines are calculated by Model III and Hu et al. [14], respectively.

dependent on the molecular weight of PEG. The interchange energy, $\tilde{\varepsilon}/k$, however, is nearly independent of the molecular weight of PEG. The $\tilde{\varepsilon}/k$ values for PEG of molecular weights 3350, 8000 and 15 000 are 164.97 K, 168.49 K and 165.73 K, respectively. As shown by these results, regardless of the molecular weight of PEG, the $\tilde{\varepsilon}/k$ value is a constant. On the other hand, r_2 values increase as the molecular weight increases because r_2 is dependent on the critical volume fraction of the polymer. The critical volume fraction of polymer is shifted to the polymer poor phase by the increase of the molecular weight of PEG.

Fig. 8 shows the phase diagram of polypropylene glycol (PPG) (Mw = 421) in water [22]. In this figure, the calculated curves by Model III and Hino et al.'s model [15] are indicated by the solid and dashed lines, respectively. The model adjustable parameter values are $r_2 = 16.601$, $\varepsilon/k = -687.89$ K, $\delta\varepsilon^H/k = 14\,529$ K and $\delta\varepsilon^S/k = 16.563$ K. Model III also well describes the closed miscibility loop phase behavior and shows improved results when compared with those of Hino et al.'s.

Fig. 9 shows the phase diagram of 2-butoxyethanol/water system [23]. The solid and dashed lines are calculated by Model III and Hu et al.'s double lattice model [14], respectively. The model adjustable parameter values of Model III are $r_2 = 215.31$, $\varepsilon/k = -424.06$ K, $\delta\varepsilon^H/k = 3681.8$ K and $\delta\varepsilon^S/k = 1.6163$ K. Model III and Hu et al.'s model agree well with experimental data, but Model III is more accurate than Hu et al.'s model. These models are based on the equal number of adjustable parameters, the number is 4. The parameters of Hu et al.'s model are r_2, ε/k, $\delta\varepsilon/k$, c_{10}. The improvement of Model III description might be due to the modified double lattice model overcoming the mathematical defect of the double lattice model.

Fig. 10 shows the phase diagram of nicotine/water system [23]. In this figure, the calculated coexistence curves by Model III, Hu et al.'s model [14] and Hino et al.'s model [15] are indicated by the solid, dashed and dotted lines, respectively. The model adjustable parameter values are $r_2 = 166.36$, $\varepsilon/k = -514.91$ K, $\delta\varepsilon^H/k = 4961.4$ K and $\delta\varepsilon^S/k = 2.5055$ K. In this system, the prediction of closed loop phase behavior using Model III is satisfactory and also shows better results than those of other models.

In our proposed model, various flexibilities of chain molecules are not included. The model implicitly assumes that all polymers have the same flexibility. Further, solvent molecules are considered to be monomers where the concept of flexibility does not apply. It is likely that this deficiency is basically responsible for the discrepancy between the proposed model and the experimental results.

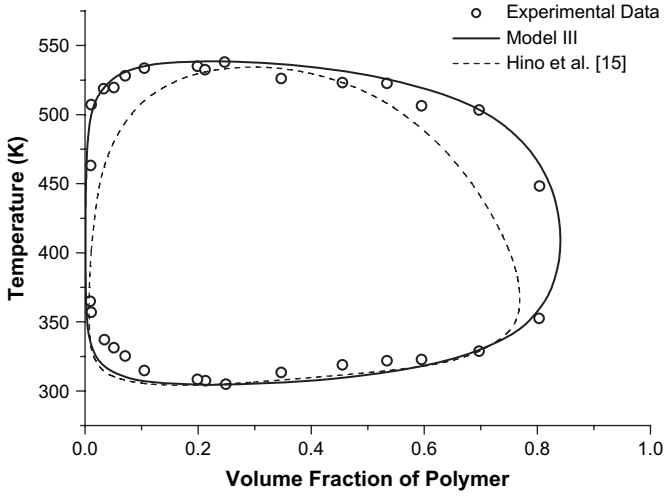

Fig. 8. Coexistence curves for PPG/water system. The open circles are experimental data [22] for PPG molecular weights of 421. The solid and dashed lines are calculated by Model III and Hino et al. [15], respectively.

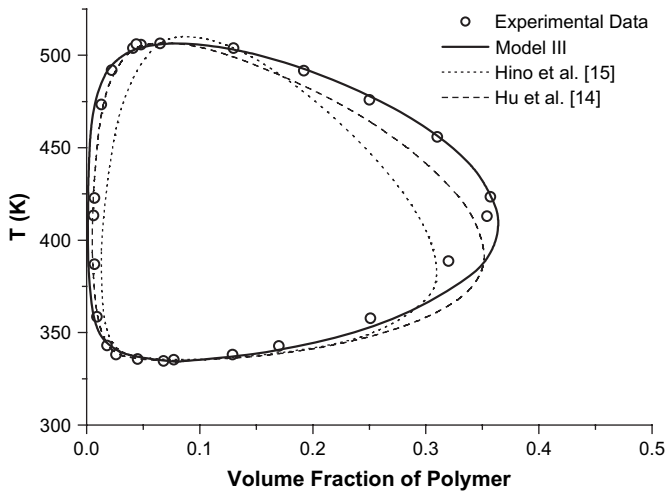

Fig. 10. Coexistence curves for nicotine/water system. The open circles are experimental data [23]. The solid, dotted and dashed lines are calculated by Model III, Hino et al. model [15], and Hu et al. model [14], respectively.

4. Conclusion

We proposed three types of models to describe liquid–liquid phase equilibria. The models are based on a modified double lattice model. Especially, to describe closed miscibility loop phase behavior, we introduce a corrected specific interaction model. We have also shown several phase diagrams of some binary polymer solutions. For those binary polymer solutions, our proposed model appears to be useful in describing and predicting the liquid–liquid equilibria using a few adjustable parameters.

Acknowledgment

This work is supported by Seoul RNBD.

References

[1] Barker JA, Fock W. Discuss Faraday Soc 1963;15:188.
[2] Wheeler JC. J Chem Phys 1975;62:433.
[3] Anderson GR, Wheeler JC. J Chem Phys 1978;69:3403.
[4] Abrams DS, Prausnitz JM. AIChE J 1975;21:116.
[5] Kim YC, Kim JD. Fluid Phase Equilib 1998;41:229.
[6] Matsuyama A, Tanaka F. Phys Rev Lett 1990;65:341.
[7] Waker JS, Vause CA. Phys Lett 1980;79A:421.
[8] Bae YC, Shim JJ, Soane DS, Prausnitz JM. J Appl Polym Sci 1998;47:1193.
[9] Yang J, Xin Q, Sun L, Liu H, Hu Y, Jiang J. J Chem Phys 2006;125(16):164506.
[10] Yang J, Peng C, Liu H, Hu Y. Fluid Phase Equilib 2006;249:192.
[11] Yang J, Yan Q, Liu H, Hu Y. Polymer 2006;47(14):5187.
[12] Yang J, Peng C, Liu H, Hu Y, Jinang J. Fluid Phase Equilib 2006;244:188.
[13] Hu Y, Lambert SM, Soane DS, Prausnitz JM. Macromolecules 1991;24:4356.
[14] Hu Y, Liu H, Soane DS, Prausnitz JM. Fluid Phase Equilib 1991;67:65.
[15] Hino T, Lambert SM, Soane DS, Prausnitz JM. AIChE J 1993;39:837.
[16] Brinke GT, Karasz FE. Macromolecules 1984;17:815.
[17] Oh JS, Bae YC. Polymer 1998;39:1149.
[18] Madden WG, Pesci AI, Freed KF. Macromolecules 1990;23:1181.
[19] Panagiotopolous AZ, Quirke N, Stapleton M, Tildesley DJ. Mol Phys 1998;63:527.
[20] Bae YC, Shim JJ, Soane DS, Prausnitz JM. Macromolecules 1991;24:4403.
[21] Flory PJ, Shultz AR. J Am Chem Soc 1952;74:4760.
[22] Muller C. Diploma thesis, University of Karlsruhe; 1991.
[23] Sorensen JM, Arlt W. Liquid–liquid equilibrium data collection (binary systems), Part 1. In: Chemistry data series, vol. V. Frankfurt am Main: DECHEMA; 1979.